Electrochemical characterization of microelectrodes used for neural interfaces

Ben Rees[1] and Mohammad Mundiwala[2]

[1] Combustion Diagnostics Laboratory
[2] Reliability Engineering and Informatics Laboratory

Keywords: Charge storage capacity, electronics, mems

Abstract. Precise evaluation of soft neural microelectrode performance and safety is crucial for successful implementation. In this work, we characterized each of the four electrode-channels of an electrode-encapsulation unit using electrochemical impedance spectroscopy (EIS), cyclic voltammetry (CV), and voltage transient (VT) measurements to evaluate its potential for neural recording and stimulation. EIS revealed an average impedance value of $5.64 \times 10^5\ \Omega$ at 1 kHz with phase profiles that approach ideal capacitive behavior at mid-to-high frequencies and trended towards resistive behavior at low frequencies, which was not expected. The average cathodic charge storage capacity (CSC_c) was 0.766 mC cm^{-2} and the average charge injection capacity (CIC) was 0.824 mC cm^{-2}, both of which indicate a strong material basis for competent and safe stimulation. The third of the four channels showed an average 62% greater CSC_c than the other three channels, highlighting the need for consistent and robust manufacturing practice.

1 Introduction

Many modern solutions to Parkinson's disease, epilepsy, spinal cord injury and depression are built on our ability to communicate with the nervous system. Among many design requirements, neural interfacing devices must effectively and safely stimulate and record electrical impulses from neural tissue. Microelectrodes require special characterization methods because their performance must span a wide range of high-charge signals without incurring damage to the surrounding tissue or the electrode itself, and must do so over long periods of time. This report provides a comprehensive characterization of the electrode channels of an electrode-encapsulation unit in order to evaluate the safety and efficacy of a new design.

The key structure of the neural interface is the formation of the electrical double layer, which is the capacitor-like attraction and repulsion of electrolyte ions at the electrode surface which spontaneously forms and transfers charge without chemical reactions occurring. This capacitive charge transfer is foundational to effective neural recording as it allows for the non-destructive sensing of minute voltage fluctuations present in neural activity. Low impedance and a phase angle approaching -90° as probed by electrochemical impedance spectroscopy (EIS) demonstrate a high-quality recording interface.

Neural stimulation requires more extreme charge transfers and therefore a different mechanism. Faradaic charge transfer, where reversible reduction-oxidation reactions occurring on the electrode surface rapidly inject charge, are ideal for effective stimulation and can be measured by the charge storage capacity (CSC) calculated from cyclic voltammetry (CV). Large CSC indicates a sizable charge reservoir which allows for sufficient charge injection that still remains within safe interface voltage potentials.

21 September 2025

The risk of damage to surrounding tissue and to the electrode itself is mitigated through the prevention of irreversible Faradaic reactions, which not only are inefficient but also corrode the electrode surface, increase the pH toxicity of the neural electrolyte solution, and may cause gas bubble formation. This is avoided by ensuring that Faradaic charge transfer does not occur at an interface voltage outside of the range -0.6 to 0.8 V, which is known as the "water window," as water hydrolysis is one of the more common deleterious irreversible Faradaic reactions. The maximum charge able to be injected while remaining within the "water window" is known as the charge injection capacity (CIC) and is analyzed via the voltage transient (VT) probed with alternating current application.

By comparing the EIS, CSC, and CIC results to benchmarks established in literature reviews such as Ref. [1], the performance and safety of each channel in our electrode- encapsulation unit is thoroughly assessed for potential implementation.

2 Data and Methods

Flexible electrodes were implanted into a flexible encapsulation via metal deposition and photolithography. The resulting electrode heads (connection sites) may be seen in Figure 1 below.

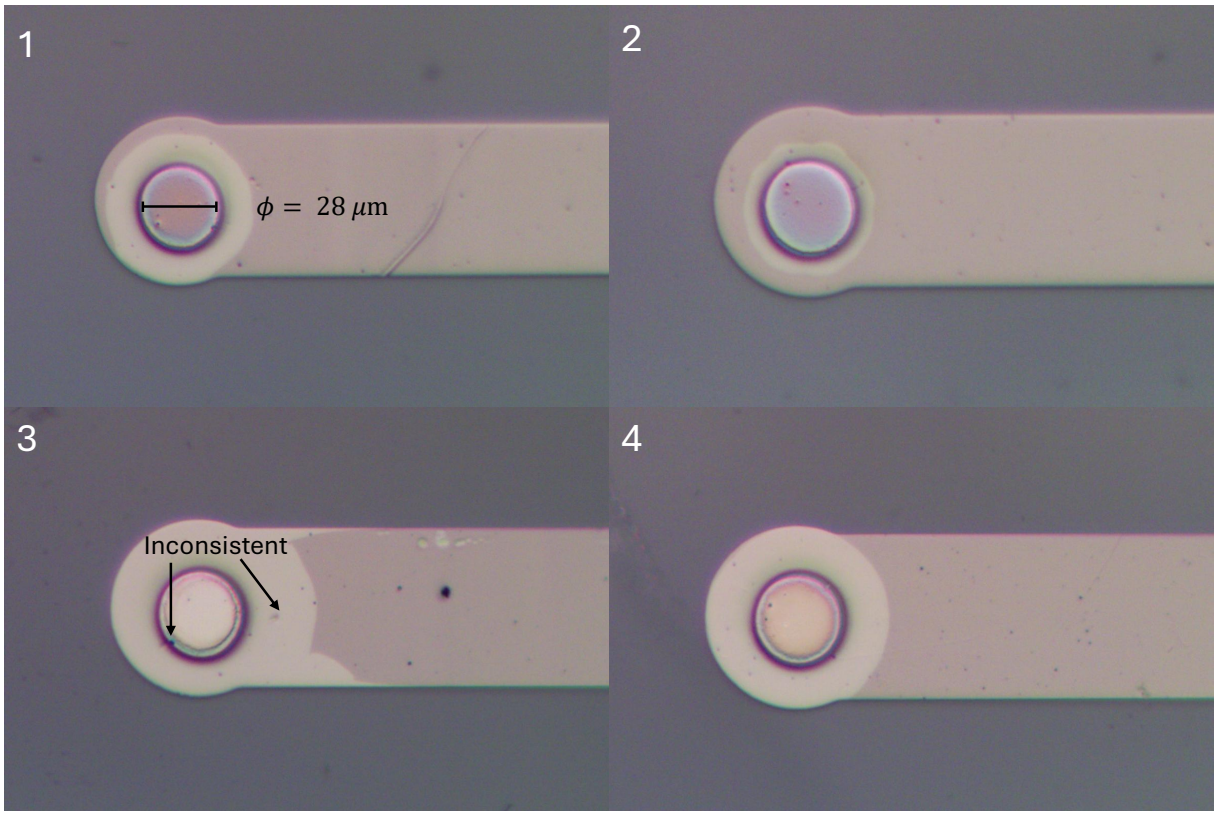

Figure 1: Electrode channel heads 1-4.

The electrode channel connection site was produced with a diameter of 28 μm. The entire encapsulation was then suspended in a simulated neural electrolyte bath, with the electrode channel head connected to a power unit and a reference signal connected to the electrolyte

bath nearby to the encapsulation. Electrical signals were then passed through the electrode-encapsulation unit to evaluate various performance metrics as is described in the sections below.

2.1 Electrochemical Impedance Spectroscopy

Electrochemical impedance spectroscopy, or EIS, is used to measure the electric impedance and phase angle frequency dependence across the electrode [1]. We span from 0.1 Hz to 100 kHz with a sinusoidal amplitude of 50 mV (small enough to assume linearity) and an initial quiet time of 2 seconds. This testing is done across 4 of the 5 electrodes in the tested unit. The resulting impedance magnitude and phase were then plotted in a Bode plot as is found in Figure 2.

The impedance at 1 kHz is especially considered due to its relevance to neural action potentials [1], falling central in the range of typical neural signals that are between 100 Hz and 10 kHz. An electrode with particularly low impedance at 1 kHz will have a favorable signal to noise ratio (SNR), detecting the more quiet action potentials from within the general electrical background noise of the brain and electrode itself.

The phase response with frequency ideally has two regions: (1) as close to -90° at low to mid frequencies as is possible, particularly at those frequencies relevant to neural signals (< 5 kHz), and (2) trending towards 0° at much higher frequencies (> 10 kHz). The former indicates electrolyte-electrode capacitive behavior at typical neuronal signal frequencies, which is ideal because it is associated with the non-Faradaic mechanism of charge transfer that is able to non-destructively sense small voltage changes. As the signal frequency gets higher and the capacitive behavior is overloaded, the latter criterion serves as a simple resistor quality measurement, with a perfect resistor showing a phase of 0°.

2.2 Cyclic Voltammetry

Cyclic voltammetry (CV) is an electrode measurement where the potential of a test electrode is swept cyclically at a constant rate between -0.6 V and 0.8 V while the current flowing between the test electrode and a counter electrode is recorded [1]. In this report we characterize the electrodes by their cathodal charge storage capacity ($\mathrm{CSC_c}$). The $\mathrm{CSC_c}$ is calculated using

$$\mathrm{CSC_c} = \frac{1}{\nu A} \int_{V_{min}}^{V_{max}} i(V)\, dV \tag{1}$$

where ν is the sweep rate (0.1 V/s), A is the area of the electrode calculated based on the electrode interface diameter, i is the measured current, and V_{min} and V_{max} are the potentials just within the water electrolysis window taken as - 0.6 V and 0.8 V, respectively. The CSC_c represents the total reservoir capacity of the electrode-encapsulation unit, with larger values indicating a higher capacity to safely inject large charges and in turn more thorough signal generation. The values were calculated from the final of 4 total loops, allowing the system to stabilize.

The resulting current was plotted against the applied potential for the four channels and may be viewed in Figure 3 shown below. The cathodic charge storage capacity was found by integrating the area graphically bounded by $i = 0$ and the internal area of the current versus applied potential curve and dividing by the scan rate and the electrode channel-head area.

2.3 Voltage Transients

Voltage transient, or VT, measurements are used to estimate the charge injection capacity, and are performed via a current-controlled stimulation pulse [1]. The transients are analyzed to determine the maximum polarization across the electrode-electrolyte interface. The voltage transient is defined by

$$\Delta V = i_c R_i + \eta_c + \eta_a + \Delta E, \tag{2}$$

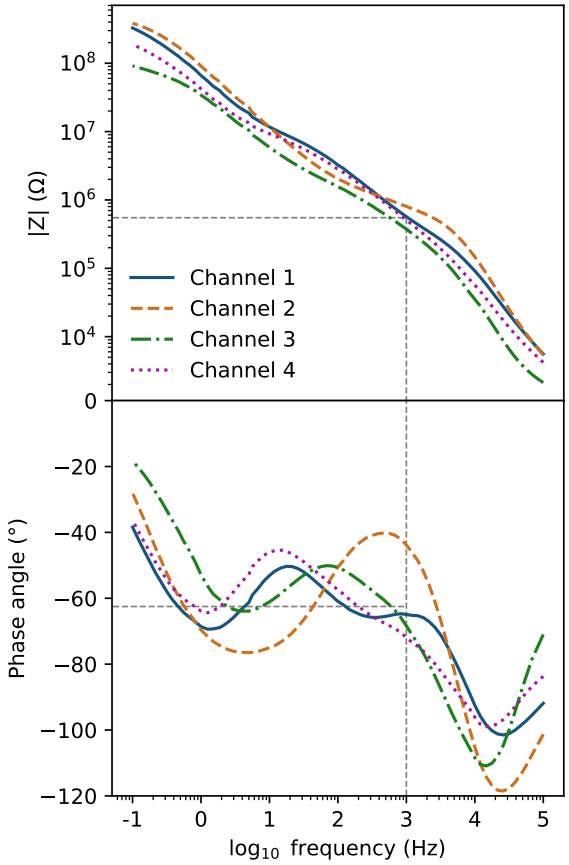

Figure 2: Bode plot- Electrochemical impedance spectroscopy results for phase angle and magnitude of impedance over frequency sweep from 0.1 Hz to 100 kHz; for frequency of 1 kHz, the mean impedance and phase angle are $5.65 \times 10^5\ \Omega$ and $-62.5°$, respectively.

where i_c is the current applied, R_s is the solution resistance, η_c and η_a are the cathodic and anodic overpotential, an ΔE is the polarization value. In this work, we take the empirical ΔE as

$$\Delta E = V_{\text{baseline}} - V_{\text{peak,cathodic}}, \tag{3}$$

and is calculated directed from transient data. Note that calculating ΔE this way includes both solution-resistance drop and electrode polarization; still, this estimate can be useful to assess safe operation within a desired window (i.e., water window).

3 Results and Discussions

3.1 EIS Results

Average impedance for the four tested channels at 1 kHz was found to be $5.64 \times 10^5\ \Omega$ with similar behavior in all electrode channels, which is a relatively high impedance compared to more ideal levels cited at 50-100 kΩ [1]. Used as a recording device, the electrode will likely experience greater background noise at this impedance level. The frequency-dependent phase response plot shows a larger discrepancy between channels, potentially indicating inconsistent encapsulation quality, non-uniform surface coating, or surface contamination on the electrodes. The physical significance of phase response differences between channels is that of more or less resistive or capacitive behavior at that particular frequency, which is an important metric for the nature of charge transfer at the electrode interface. The overall phase response of all four channels is unexpected - ideal behavior for signal measurement is capacitive (near -90°) at low

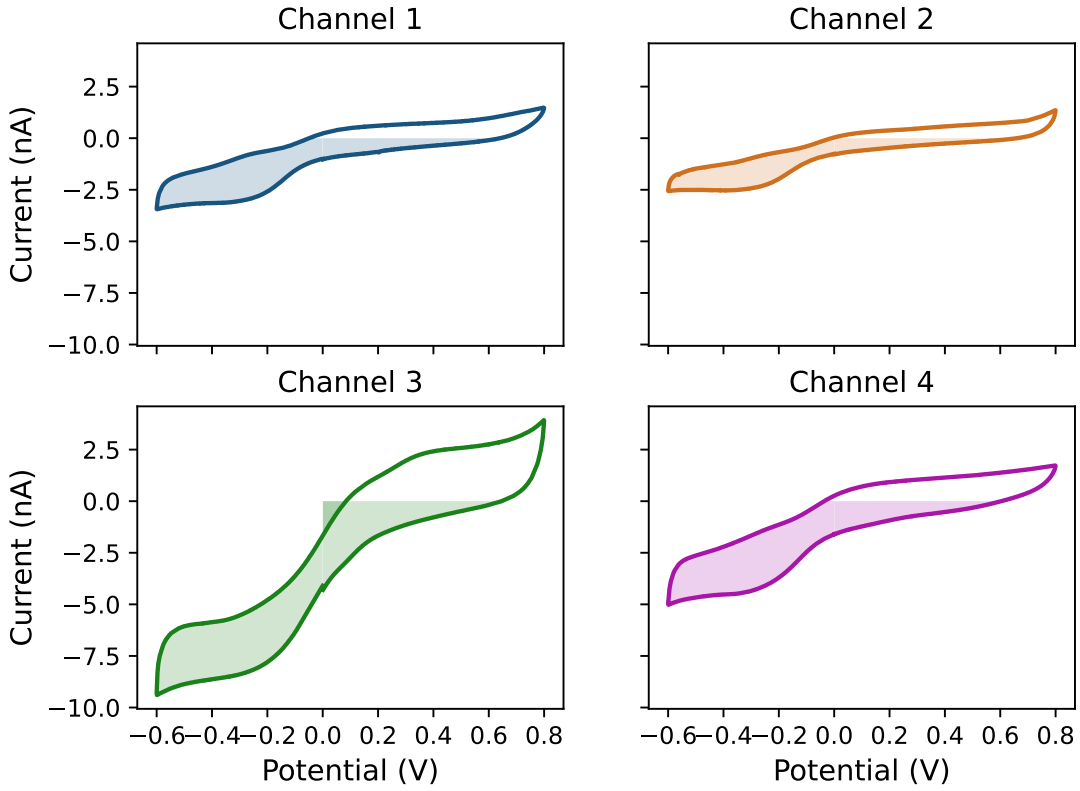

Figure 3: Cyclic voltammetry plot for the final loop that was recorded; shaded area indicates the cathodic region used to calculate the charge storage capacity

frequencies ($<$ 5 kHz) and is purely resistive (near 0°) at higher frequencies ($>$ 10 kHz). Phase response decreasing to -110° and beyond at high frequencies suggests the influence of inductive artifacts from the wiring in the test setup as the impedance from the electrode-electrolyte interface becomes less dominant.

3.2 CV Results

The CV results are plotted in Figure 3 and the calculated CSC_c for each electrode is given in Table 1. The charge storage capacity is adequate for neural stimulation in all channels, but is abnormally high in the third channel. Similar to the EIS phase response results, this anomalously high value along with the distinct connection site appearance able to be seen in Figure 1 suggests inconsistent encapsulation quality, inconsistent surface coating, or surface contamination, all of which could lead to the high value of CSC_c recorded.

Channel	**CIC** ($\frac{mC}{cm^2}$)	**CSC$_c$**($\frac{mC}{cm^2}$)
1	0.763	0.510
2	0.747	0.376
3	0.974	1.449
4	0.812	0.728

Table 1: **CV and VT results**. Charge injection capacity and charge storage capacity derived from voltage transient data and cyclic voltammetry integration, respectively.

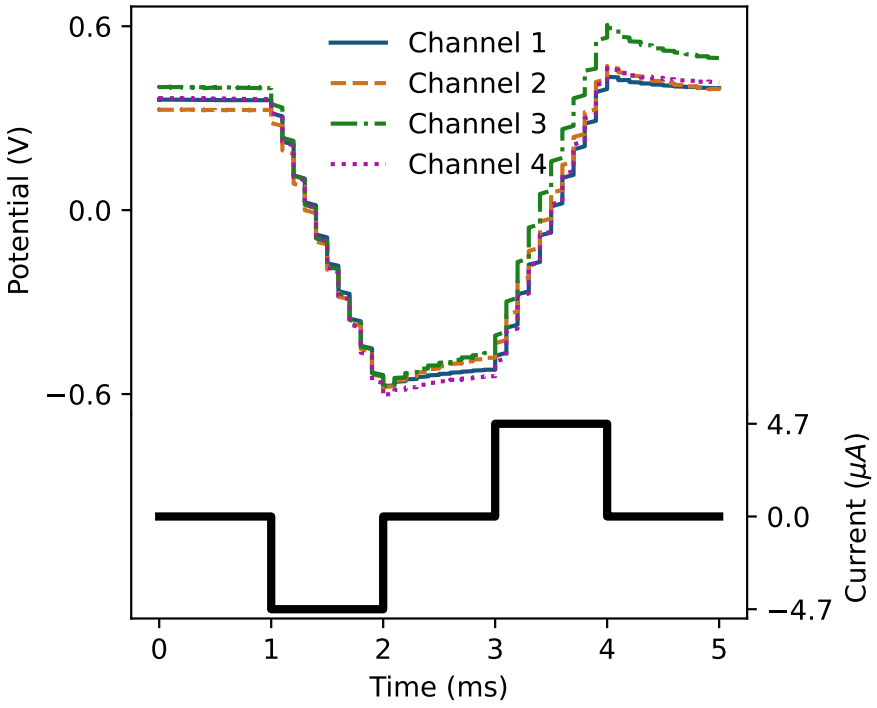

Figure 4: Voltage transient of a single cycle for channels 1-4. Note that the input current of only channel 1 is shown; channels 2-4 have amplitudes of 4.6, 6, and 5 μA, respectively.

3.3 VT Results

More useful than the CSC_c, however, is the charge injection capacity (CIC) as measured from VT as it simulates stimulation transients and measures the true safe limit of the device to inject charge. The applied current profile is shown in the bottom of Figure 4 and the resulting voltage transients may be seen above it. The increase in applied current had to be curtailed due to oxidation accumulation at the electrode surface, which led to positive voltages during the reset phase that got too close to the upper voltage limit. The calculated CIC is therefore short of what truly maximum polarization would allow. The mean polarization ΔE across the four electrodes was 0.923 ± 0.034 V; channel-level results are summarized in Table 2. From Figure 4 we can see the fast drop during the cathodic step and the fast rise during the anodic step, as expected. The peak cathodic voltage remains within the acceptable water window across all electrodes which is a good sign. The variance across electrodes is minimal and suggests that contact surfaces are consistent. Under the tested current pulses, the electrode behavior is classified as reversible since the potential returns to the same baseline after each cycle and because the charge and discharge plots (Figure 4) is capacitive in nature.

Channel	**Baseline** (V)	**Peak Cathodic** (V)	**Total** ΔE (V)
1	0.375	-0.579	0.954
2	0.344	-0.581	0.925
3	0.428	-0.587	1.015
4	0.385	-0.607	0.992
mean	0.383	−0.589	0.971

Table 2: **Voltage transient results.** Baseline voltage, peak cathodic voltage, and total voltage drop (ΔE) across four electrodes. Mean values show that the total drop exceeds the acceptable threshold .

4 Conclusion

In this report we detail and demonstrate a framework to characterize microelectrodes used in our small device of interest. Based on EIS, CV, and VT results, we show that the device can safely inject charges appropriate for neural stimulation within a safe voltage window and that charge transfer is reversible. Three of four channels showed reproducible metrics (CIC and CSC_c) which indicates that the fabrication process is decent but has room for improvement. Channel three seems to be distinct from the others which likely means its effective surface area was larger than the rest or that its surface composition was inconsistent. If electrode surfaces are not uniform due to contamination or roughness, channels will store and inject different amounts of charge. By testing identical small devices, the results of this study would be more conclusive and a more informed decision could be made to improve future electrode design.

The EIS results showed that at phase angles at low frequencies did not approach the ideal -90° and actually dropped to -110 °, which is not realistic for a passive electrode. These results likely reflect inductive artifacts from the test setup circuitry, rather than the true electrode behavior. Despite this, the impedance magnitudes were within the expected order at 1 kHz, which agrees with our expectations of neural electrodes. It may be possible that the data acquisition methods for the EIS are responsible for the unexpected phase response. To address this, the experiments were performed in a Faraday cage to prevent outside electrical noise; future experiments could use shorter connection wires, twisted electrode leads to reduce inductive fields, or shielded coaxial cables to prevent resistance effects from the connection itself.

Another limitation in this study could be from the simulated electrolyte solution which greatly simplifies true intracellular fluid that might be seen with in-vivo testing. The study may also benefit from testing different scan rates and pulse width values for CSC_c and CIC calculations. Although results fell within acceptable ranges, testing more conditions might provide a more thorough characterization of the device.

Availability of data and code

Our code is available at the following URL: https://github.com/mohammadmundiwala/Flexible-Electronics/tree/main/lab-1.

References

[1] Stuart F Cogan. Neural stimulation and recording electrodes. *Annu. Rev. Biomed. Eng.*, 10(1):275–309, 2008.